Bioorganic & Medicinal Chemistry 20 (2012) 5483–5495

Contents lists available at SciVerse ScienceDirect

Bioorganic & Medicinal Chemistry

journal homepage: www.elsevier.com/locate/bmc

UDP made a highly promising stable, potent, and selective P2Y6-receptor agonist upon introduction of a boranophosphate moiety ☆

Tamar Ginsburg-Shmuel [a,†], Michael Haas [b,†], Djordje Grbic [c], Guillaume Arguin [c], Yael Nadel [a], Fernand-Pierre Gendron [c], Georg Reiser [b,†], Bilha Fischer [a,†,*]

[a] Department of Chemistry, Gonda-Goldschmied Medical Research Center, Bar-Ilan University, Ramat-Gan 52900, Israel
[b] Institute for Neurobiochemistry, Faculty of Medicine, Otto von Guericke University, Leipziger Str. 44, D-39120 Magdeburg, Germany
[c] Canadian Institute of Health Research Team on the Digestive Epithelium, Département d Anatomie et de Biologie Cellulaire, Faculte de Medecine et des Sciences de la Sante, Universite de Sherbrooke, 3001 12th Avenue North, Sherbrooke, Quebec, Canada

ARTICLE INFO

Article history:
Received 16 May 2012
Revised 19 July 2012
Accepted 20 July 2012
Available online 2 August 2012

Keywords:
Nucleotides
$P2Y_6$-receptor
UDP

ABSTRACT

$P2Y_6$ nucleotide receptor ($P2Y_6$-R) plays important physiological roles, such as insulin secretion and reduction of intraocular pressure. However, this receptor is still lacking potent and selective agonists to be used as potential drugs. Here, we synthesized uracil nucleotides and dinucleotides, substituted at the C5 and/or P_α position with methoxy and/or borano groups, **18–22**. Compound **18A**, R_p isomer of 5-OMe-UDP(α-B), is the most potent and $P2Y_6$-R selective agonist currently known (EC_{50} 0.008 μM) being 19-fold more potent than UDP and showing no activity at uridine nucleotide receptors, $P2Y_2$- and $P2Y_4$-R. Analogue **18A** was highly chemically stable under conditions mimicking gastric juice acidity ($t_{1/2}$ = 16.9 h). It was more stable to hydrolysis by nucleotide pyrophosphatases (NPP1,3) than UDP (15% and 28% hydrolysis by NPP1 and NPP3, respectively, vs 50% and 51% hydrolysis of UDP) and metabolically stable in blood serum ($t_{1/2}$ = 17 vs 2.4, 11.9, and 21 h for UDP, 5-OMe-UDP, and UDP(α-B), respectively). This newly discovered highly potent and physiologically stable $P2Y_6$-R agonist may be of future therapeutic potential.

1. Introduction

The members of the P2 receptor (P2R) superfamily, consisting of ligand-gated ion channels (P2X-Rs) and G protein-coupled receptors (P2Y-Rs), are activated by endogenous extracellular nucleotides.[1] Eight human P2Y-Rs subtypes are known so far ($P2Y_1$, $P2Y_2$, $P2Y_4$, $P2Y_6$, $P2Y_{11}$–$P2Y_{14}$). The $P2Y_{1,2,11-13}$ receptors are activated by adenine nucleotides (adenosine 5′-triphosphate, ATP, **1**, or adenosine 5′-diphosphate ADP, **2**). $P2Y_{2,4,6}$-Rs are P2Y-R subtypes that are activated by uracil nucleotides, while the $P2Y_2$-R is activated by **1** as well as uridine 5′-triphosphate, UTP, **3**, with similar potency. $P2Y_4$-R is activated only by **3** and $P2Y_6$-R is a uridine 5′-diphosphate, UDP, **4**, receptor (Fig. 1). Recently, it was reported that $P2Y_{14}$-R is also activated by **4** as well as UDP-glucose.[2]

The $P2Y_6$-R is widely spread in the human body and has many physiological roles. It has been shown to be expressed in macrophages.[3] In addition, it has been found in aortic endothelial and smooth muscle cells and proved to be involved in both the direct contraction and endothelium-dependent relaxation of the aorta.[3] Also, microglia express $P2Y_6$ receptors that function as a sensor of phagocytosis. Therefore, the activation of $P2Y_6$ receptors by agonists would be a key event in initiating the clearance of dying cells or debris in the central nervous system. Thus, a $P2Y_6$-R agonist could be beneficial in Alzheimer's disease.[4] Also, $P2Y_6$-R expression is increased by the stress associated with intestinal inflammation.[5] Therefore, a $P2Y_6$-R antagonist may be helpful for the treatment of inflammatory bowel diseases.

$P2Y_6$ receptor agonists have been reported to counteract apoptosis induced by tumor necrosis factor α in astrocytoma cells stably expressing the human $P2Y_6$ receptor.[6] The attenuation of ischemia/reperfusion injury in vivo in mouse skeletal muscle by $P2Y_6$ receptor activation has also been reported.[7] Selective stimulation of the $P2Y_6$ receptor increases insulin secretion that accompanies intracellular calcium release, suggesting potential application for these receptor ligands in the treatment of diabetes.[8] In addition, **4** can selectively activate $P2Y_6$ receptors involved in the reduction of intraocular pressure.[9]

Lately, the structure–activity relationship of $P2Y_6$-R agonists and antagonists, and molecular modeling of the $P2Y_6$-R have been extensively investigated.[10–14] $P2Y_6$ receptor is still lacking potent and selective synthetic agonists and antagonists. To date the development of agonists for the $P2Y_6$-R included modification of the phosphate chain, ribose ring, and base of **4** (Fig. 2).[15] Different

☆ Patent is pending.

* Corresponding author. Tel.: +972 3 5318303; fax: +972 3 6354907.
E-mail address: bilha.fischer@biu.ac.il (B. Fischer).
† These authors contributed equally.

0968-0896/$ - see front matter © 2012 Elsevier Ltd. All rights reserved.
http://dx.doi.org/10.1016/j.bmc.2012.07.042

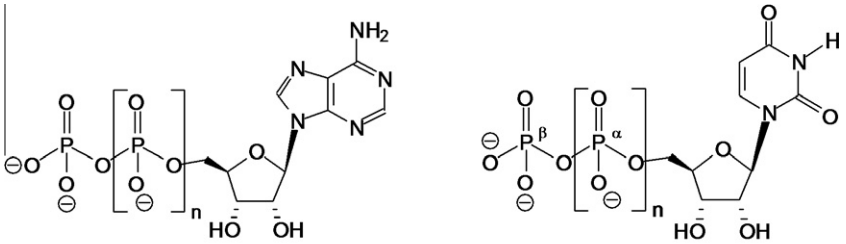

Figure 1. Endogenous agonists of P2Y-Rs.

uracil modifications have been performed over the last years in an attempt to identify agonists which will prove to be more potent than the endogenous ligand **4**.[13,16,17]

Thus, UDP-β-S, **5**, was found to be ~sixfold more potent than **4** in activation of the $P2Y_6$-R.[11] Furthermore, it has been shown that the terminal thiophosphate moiety increases stability towards nucleotidases. 5-Br-UDP, **6**, and 5-iodo-UDP (MRS2693), **7**, were found to be equipotent to **4**.[14,18] 5-OMe-UDP, **8**, was recently reported by us to be a potent and selective $P2Y_6$-R agonist.[16] Modification on the N3 of the uracil ring led to the potent agonist, 3-phenacyl-UDP, **9**.[10] α,β-Methylene-UDP, **10**, and 5-Br-β,γ-dichloromethylene-UTP, **11**, were prepared to enhance chemical and enzymatic stability.[10,17] Maruoka et al. recently reported the development of N^4 modified cytidine analogues as $P2Y_6$-R agonists, for example, N^4-benzyloxy-CDP, **12**, and N^4-methoxy-CDP, **13**.[13] The dinucleotide Up_3U, **14**, is equipotent to the endogenous agonist,[17] while the dinucleoside triphosphate INS48823, **15**, was found to be a potent and stable agonist.[19] Assessment of the pharmacological activity of (*S*)-methanocarba-UDP, **16**, together with molecular modeling studies, have shown that while the $P2Y_2$-R and $P2Y_4$-R prefer the *N* (Northern) conformation of the ribose ring, the *S* (Southern) conformation is the one preferred by the $P2Y_6$-R.[12,14,20] Only one irreversible antagonist of the $P2Y_6$-R has been reported so far, MRS2578, **17**.[21]

The therapeutic potential of nucleotides is limited because they are degraded by extracellular enzymes,[22] which reduces their potency, efficacy, and duration of action. Nucleotides are hydrolyzed enzymatically by the ecto-nucleoside-triphosphate diphosphohydrolase family of ectonucleotidases (i.e., e-NTPDase and alkaline phosphatases)[23] and ecto-nucleotide pyrophosphatases/phosphodiesterases (i.e., e-NPPs).[24,25] Therefore, there is a need for the identification of enzymatically and chemically stable nucleotide scaffolds that can be used to develop selective and potent P2Y-R agonists.

Several methods to improve the stability of nucleotides via the use of phosphate bioisosters of nucleotides include thiophosphate,[26–29] phosphonate,[30–36] phosphoramidate[37] and boranophosphate[23,38] analogues. A second strategy for enhancing stability of potential P2Y-Rs agonists is the use of dinucleotides, such as diuridine triphosphates, which show greater stability than analogues of mononucleotides,[39,40] Indeed, dinucleotides have been successfully developed before as $P2Y_2$-R agonists. Thus, Up_4U (INS365, Diquafosol) and Up_4dC (INS37217, Denufosol), have been clinically tested for the treatment of dry eye disease and cystic fibrosis, respectively, however, both compounds did not show satisfying results at phase 3 clinical trial.[1,41]

Here, we describe the design and synthesis of analogues **18–22** and their activity and selectivity at the $P2Y_6$ receptor. Specifically, we report the identification of 5-OMe-UDP(α-B)-R_p isomer, **18A**, as a most potent, stable and selective $P2Y_6$-R agonist. In addition, we report on the chemical stability of **18A** in pH mimicking gastric juice acidity, its resistance to hydrolysis by NPP1,3, and its stability in human blood serum. Finally, we determine the absolute configuration of the promising agonist **18A** and analyze the beneficial effect of the borano moiety with regard to activity and selectivity of studied borano-analogues versus related compounds.

2. Material and method

2.1. Chemistry

2.1.1. General

All air and moisture sensitive reactions were carried out in flame-dried, argon flushed, two-neck flasks sealed with rubber septa. All reactants in moisture sensitive reactions were dried overnight in a vacuum oven, and the reagents were introduced by syringe. Progress of reactions was monitored by TLC on precoated Merck silica gel plates (60F-254). Visualization was accomplished by UV light. Flash chromatography was carried out on silica gel (Davisil Art. 1000101501). All commercial reagents were used without further purification, unless otherwise noted. All phosphorylation reactions were carried out in flame-dried, argon-flushed, two-neck flasks sealed with rubber septa. Nucleosides were dried in-vacuo overnight. Proton Sponge® was kept in a desiccator. Phosphorus oxychloride was distilled and kept under nitrogen.[42] Bpi was prepared according to literature.[42] Tri-*n*-butylammonium pyrophosphate solution were prepared as described previously.[43] The preparation of the tri-*n*-butylammonium-tri-*n*-octylammonium and the bis(trioctylammonium) 5′-monophosphate 5-OMe-uridine salts were achieved by eluting the uridine nucleotide derivative (obtained after LC separation) through an activated Dowex-H^+-form using deionized water to an ice-cooled EtOH solution containing 1 equiv tri-*n*-octylamine and 1 equiv tri-*n*-butylamine. The preparation of the tetra-*n*-butylammonium 5′-diphosphate 5-OMe-uridine salt was achieved by eluting the uridine nucleotide derivative (obtained after LC separation) through a CM Sephadex previously washed with an excess of tetrabutylammonium aqueous solution. 5-Methoxy uracil, 5-methoxy-uridine, **24**, and 2′,3′-*O*-methoxymethylidene-5-OMe-uridine, **25**, were prepared according to literature.[44–47] 5-OMe-UMP, **23**, and 5-OMe-UDP, **8**, were prepared as previously described.[44] pH measurements were performed with a Metrohm pH electrode and a Metrohm 827 pH lab pH meter. Compounds were characterized by NMR using Bruker AC-200, DPX-300, or DMX-600 spectrometers. ^1H NMR spectra were recorded at 200, 300, or 600 MHz. Chemical shifts are expressed in ppm downfield from Me_4Si (TMS), used as an internal standard. Nucleotides were characterized also by ^{31}P NMR in D_2O, using 85% H_3PO_4 as an external reference on Bruker AC-200 and DMX-600 spectrometers. High resolution mass spectra were recorded on an AutoSpec Premier (Waters UK) spectrometer by chemical ionization. Nucleotides were analyzed under ESI conditions on a Q-TOF micro-instrument

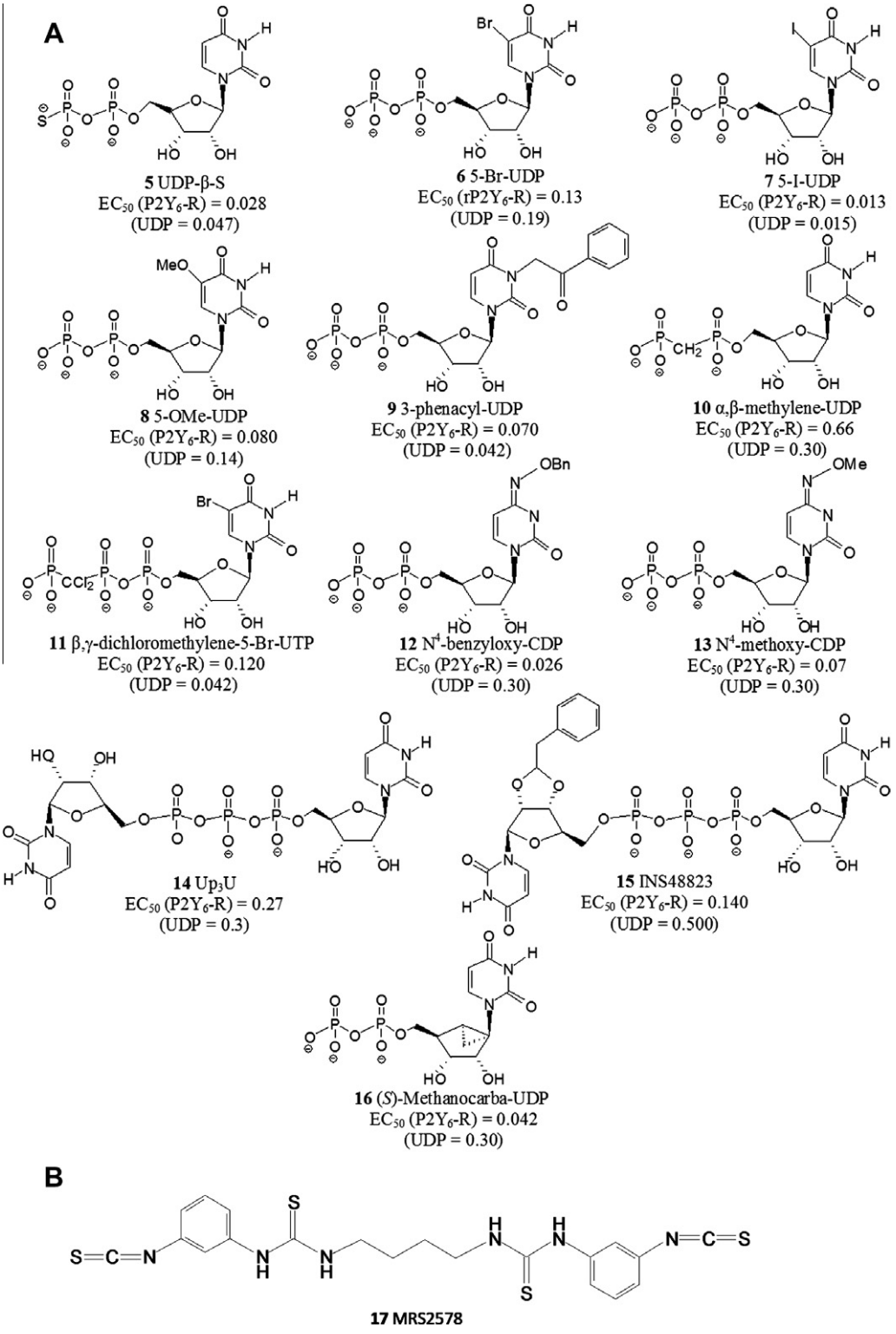

Figure 2. (A) Known $P2Y_6$-R agonists and their EC_{50} values (in μM), as compared to those of **4**. (B) A $P2Y_6$-R antagonist.

(Waters, UK). Primary purification of the nucleotides was achieved on a LC (Isco UA-6) system using a Sephadex DEAE-A25 column, swollen in 1 M $NaHCO_3$ at room temperature for 1 day. The resin was washed with deionized water before use. The LC separation was monitored by UV detection at 280 nm. A buffer gradient of NH_4HCO_3 was applied as detailed below. Final purification of the nucleotides was achieved on an HPLC (Hitachi Elite LaChrome) system, using a semi-preparative reverse-phase column (Gemini 5u C-18 110A, 250 × 10.00 mm, 5 micron, Phenomenex, Torrance, USA). The purity of the nucleotides was evaluated with an analytical reverse-phase column system (Gemini 5u C-18 110A, 150 mm × 4.60 mm; 5 μm; Phenomenex, Torrance, CA) using two solvent systems: solvent system I, (A) 100 mM triethylammonium acetate (TEAA), pH 7: (B) CH_3CN; solvent system II, (A) 10 mM PBS

buffer, pH 7.4: (B) CH_3CN. The details of the solvent system conditions used for the separation of each product are given below. The purity of the nucleotides was generally ⩾95%.

2.2. 2′,3′-*O*-Methoxymethylidene-5-OMe-uridine (25)

A suspension of 5-OMe-uridine, **24**, (300 mg, 1.09 mmol) and *p*-TsOH (catalytic amount) in trimethyl orthoformate (1.09 mL, 9.85 mmol, 9 equiv) was prepared in a flamed-dried, nitrogen-flushed two-necked round bottom flask, and stirred at rt. After 24 h the solution became almost clear and TLC ($CHCl_3$:MeOH 8:2) showed two less polar spots and the complete disappearance of the starting material. Dowex (weak base) was added (0.31 g, 1.09 mmol, 1 equiv) and the mixture was stirred at rt for 3 h. The liquid was decanted and the MeOH was used for washes. The solution was evaporated to give an oil-like residue. Co evaporations with ether were done and a white solid was obtained (a mixture of two diastereomers: 331.8 mg, 96.3%).

2.2.1. Characterization of 2′,3′-*O*-methoxymethylidene-5-OMe-uridine (25)

^{1}H NMR (DMSO-d_6, 300 MHz): δ 11.54 (br s, 1H, NH), 7.46, 7.44 (2s, 1H, H-6), 6.101, 6.01 (2s, 1H, C*H*-OCH_3), 6.00, 5.86 (2d, J = 2.9 Hz, and J = 2.7 Hz, H-1′, 1H), 5.21, 5.17 (2 m, 1H, OH-5′), 4.99–5.05 (m, 2H, H-2′), 4.88, 4.82 (2dd, J = 6.6, 3.4 Hz and J = 7.6, 3.8 Hz, 1H, H-3′), 4.18 and 4.09 (2 m, 1H, H-4′), 3.58–3.66 (m, 2H, H-5′ and H-5″), 3.606 (s, 3H, C–O*CH*$_3$), 3.30, 3.21 (2s, 3H, CH–O*CH*$_3$) ppm. HR MALDI (positive) calcd for $C_{12}H_{16}N_2Na_1O_8$ 339.080 found 339.080.

2.3. Preparation of 5-OMe-uridine-5′-O-(α-boranodiphosphate) (18)

A solution of 2′,3′-*O*-methoxymethylidene 5-OMe-uridine, **25**, (327.1 mg, 1.03 mmol) in dry DMF (2 mL) was prepared in a flame-dried, argon flushed, two-neck flask. Dry pyridine (0.42 mL, 5.17 mmol, 5 equiv) and a solution of 2-Cl-1,3,2-benzdioxaphosphorin-4-one (230.4 mg, 1.14 mmol, 1.1 equiv) in dry dioxane (2 mL) were added and the solution was stirred at rt for 10 min. Then, a mixture of 1 M $(Bu_3NH^+)_2P_2O_7H_2^{-2}$ in DMF (1.55 mL, 1.55 mmol, 1.5 equiv) and Bu_3N (0.99 mL, 4.14 mmol, 4 equiv) was added and the solution turned turbid and then clear again. Then, a 2 M solution of BH_3–SMe_2 complex in THF (5.17 mL, 10.34 mmol, 10 equiv) was added. After 15 min, ethylene diamine (0.35 mL, 5.17 mmol, 5 equiv) was added and a white precipitate was formed. After an hour at rt, the reaction was quenched with distilled water (1.4 mL) and the clear solution was evaporated and freeze-dried. TLC (isopropanol:25% NH_4OH:H_2O 11:2:7) of the crude material showed a main polar product (R_f 0.35). The methoxymethylidene protecting group was removed by acidic hydrolysis (10% HCl solution was added until pH 2.3 was obtained). After 3 h at rt, the pH was rapidly raised to 9 by addition of 24% NH_4OH solution (pH 11), and the solution was stirred at rt for 45 min and then freeze-dried. The semisolid obtained after freeze-drying was chromatographed on an activated Sephadex DEAE-A25 column. The resin was washed with deionized water and loaded with the crude residue dissolved in a minimal volume of water. The separation was monitored by UV detection (ISCO, UA-6) at 280 nm. A buffer gradient of 0–0.2 M NH_4HCO_3 (200 mL of each solution) followed by a second buffer gradient of 0.2–0.4 M NH_4HCO_3 (200 mL of each solution) were applied. The different fractions were pooled and freeze-dried three times to yield a white solid. Final separation of the diastereomers and purification of the relevant fractions was carried out on an HPLC system, using a semi-preparative reverse-phase column, under the conditions described below. The purity of the nucleotides was evaluated on an analytical reverse-phase column system, in two solvent systems as described in Supplementary data. Finally, aqueous solutions of the products were passed through a Dowex 50WX8-200 ion-exchange resin Na^+-form column and the products were eluted with deionized water to obtain the corresponding sodium salts after freeze-drying.

2.3.1. Separation of 5-OMe-uridine-5′-*O*-(α-boranodiphosphate) (18A and 18B)

The separation of analogue **18** diastereoisomers, **18A** and **18B**, was accomplished using a semipreparative reverse-phase Gemini 5u column and isocratic elution with 94:6 (A) 100 mM TEAA, pH 7: (B) CH_3CN at a flow rate of 5 mL/min. Fractions containing purified isomers [Rt 8.97 min (**18A**); 13.45 min (**18B**) isomer)] were collected and freeze-dried. Excess buffer was removed by repeated freeze-drying cycles, with the solid residue dissolved each time in deionized water. Diastereoisomers **18A** and **18B** were obtained in 50.9% overall yield (253.5 mg) after LC separation.

2.3.2. Characterization of 5-OMe-uridine-5′-*O*-(α-boranodiphosphate) (18A)

^{1}H NMR (D_2O; 600 MHz): δ 7.39 (s, 1H, H-6), 5.99 (d, J = 5.6, 1H, H-1′), 4.45 (t, J = 5.5, 1H, H-3′), 4.40 (t, J = 4.7, 1H, H-2′), 4.30 (m, 1H, H-5′), 4.26 (m, 1H, H-4′), 4.09 (m, 1H, H-5″), 3.81 (s, 3H, CH_3), 0.39 (m, 3H, BH_3) ppm. ^{31}P NMR (240 MHz, D_2O) δ: 80.43 (m, 1P, P_α-BH_3), −7.16 (d, J = 29.5 Hz, 1P, P_β) ppm. HR MALDI (negative) calcd for $C_{10}H_{18}B_1N_2O_{12}P_2$ 431.042 found 431.043. Purity data obtained on an analytical column: 94.5% and 95.3% purity using solvent system I and II, respectively.

2.3.3. Characterization of 5-OMe-uridine-5′-*O*-(α-boranodiphosphate) (18B)

^{1}H NMR (D_2O; 700 MHz): δ 7.37 (s, 1H, H-6), 6.02 (d, J = 6.5, 1H, H-1′), 4.42 (dd, J = 6.5, 5, 1H, H-2′), 4.37 (dd, J = 5, 3, 1H, H-3′), 4.28 (m, 1H, H-4′), 4.25 (m, 1H, H-5′), 4.09 (m, 1H, H-5′), 3.81 (s, 3H, CH_3), 0.36 (m, 3H, BH_3) ppm. ^{31}P NMR (240 MHz, D_2O) δ: 80.83 (m, 1P, P_α-BH_3), −7.51 (d, J = 32.4 Hz, 1P, P_β) ppm. HR MALDI (negative) calcd for $C_{10}H_{18}B_1N_2O_{12}P_2$ 431.042 found 431.043. Purity data obtained on an analytical column: 95.4% and 95.1% purity using solvent system I and II, respectively.

2.4. Preparation of 5-OMe-uridine-5′-*O*-(α-boranotriphosphate) (19)

This analogue was obtained as a by-product from the above described synthesis of **18**. After LC separation, the relevant fractions were pooled and freeze-dried three times to yield a white solid. Final separation of the diastereomers and purification of the relevant fractions was carried out on an HPLC system, using a semi-preparative reverse-phase column, under the conditions described below. The purity of the nucleotides was evaluated on an analytical reverse-phase column system, in two solvent systems as described in Supplementary data. Finally, aqueous solutions of the products were passed through a Dowex 50WX8-200 ion-exchange resin Na^+-form column and the products were eluted with deionized water to obtain the corresponding sodium salts after freeze-drying.

2.4.1. Separation of 5-OMe-uridine-5′-*O*-(α-boranotriphosphate) (19A and 19B)

The separation of analogue **19** diastereoisomers, **19A** and **19B**, was accomplished using a semipreparative reverse-phase Gemini 5u column and isocratic elution with 93:7 (A) 100 mM TEAA, pH 7: (B) CH_3CN at a flow rate of 5 mL/min. Fractions containing purified isomers [Rt 6.15 min (**19A**); 9.22 min (**19B**) isomer)] were collected and freeze-dried. Excess buffer was removed by repeated freeze-drying cycles, with the solid residue dissolved each time

in deionized water. Diastereoisomers **19A** and **19B** were obtained in 8.66% overall yield (51.7 mg) after LC separation.

2.4.2. Characterization of 5-OMe-uridine-5′-*O*-(α-boranotriphosphate) (19A)

^{1}H NMR (D_2O; 200 MHz): δ 7.32 (s, 1H, H-6), 6.00 (d, J = 5.5, 1H, H-1′), 4.38 (m, 2H, H-2′, H-3′), 4.26 (m, 2H, H-4′, H-5′), 4.08 (m, 1H, H-5″), 3.78 (s, 3H, CH_3), 0.39 (m, 3H, BH_3) ppm. ^{31}P NMR (81 MHz, D_2O) δ: 84.51 (m, 1P, P_α-BH_3), −10.33 (d, J = 19.8 Hz, 1P, P_γ), −22.48 (dd, J = 29.4, 19.8 Hz, 1P, P_β) ppm. HR MALDI (negative) calcd for $C_{10}H_{19}BN_2O_{15}P_3$ 511.009 found 511.009. Purity data obtained on an analytical column: 94.3% and 94.1% purity using solvent system I and II, respectively.

2.4.3. Characterization of 5-OMe-uridine-5′-*O*-(α-boranotriphosphate) (19B)

^{1}H NMR (D_2O; 200 MHz): δ 7.32 (s, 1H, H-6), 6.00 (d, J = 6.1, 1H, H-1′), 4.38 (m, 2H, H-2′, H-3′), 4.24 (m, 2H, H-4′, H-5′), 4.10 (m, 1H, H-5″), 3.78 (s, 3H, CH_3), 0.37 (m, 3H, BH_3) ppm. ^{31}P NMR (81 MHz, D_2O) δ: 84.58 (m, 1P, P_α-BH_3), −10.20 (d, J = 19.5 Hz, 1P, P_γ), −22.46 (dd, J = 33.3, 19.5 Hz, 1P, P_β) ppm. HR MALDI (negative) calcd for $C_{10}H_{19}BN_2O_{15}P_3$ 511.009 found 511.009. Purity data obtained on an analytical column: 96.9% and 95.3% purity using solvent system I and II, respectively.

2.5. Preparation of Di-(5-OMe)-uridine 5′,5″-P^1,P^3,α-boranotriphosphate (20)

The tri-*n*-butylammonium-tri-*n*-octylammonium 5-OMe-uridine monophosphate salt (0.201 mmol) was dissolved in dry DMF (0.4 mL), and added to a flame-dried, nitrogen-flushed two-neck round bottom flask containing CDI (162.8 mg, 1.005 mmol, 5 equiv). The reaction was stirred at rt. After 2 h TLC (NH_4OH:-H_2O:2-propanol 2:7:11) showed the presence of a less polar product (R_f 0.62) and the complete disappearance of the starting material. (R_f 0.35). MeOH (0.07 mL, 1.81 mmol, 9 equiv) was added to destroy CDI leftovers, and, after 10 min, a solution of **18** (0.201 mmol, 1 equiv) in dry DMF (1 mL) and $MgCl_2$ (76 mg, 0.804 mmol, 4 equiv) were added. The solution was stirred at rt and TLC monitoring after 24 h showed the presence of a more polar product (R_f 0.41) and the complete disappearance of intermediate **30**. The solution was freeze-dried after the addition of water. The semisolid obtained after freeze-drying was chromatographed on an activated Sephadex DEAE-A25 column. The resin was washed with deionized water and loaded with the crude residue dissolved in a minimal volume of water. The separation was monitored by UV detection (ISCO, UA-6) at 280 nm. A buffer gradient of 0–0.2 M NH_4HCO_3 (200 mL of each solution) followed by a second buffer gradient of 0.2–0.4 M NH_4HCO_3 (250 mL of each solution) were applied. The different fractions were pooled and freeze-dried three times to yield a white solid. Final separation of the diastereomers and purification of the relevant fractions was carried out on an HPLC system, using a semi-preparative reverse-phase column, under the conditions described below. The purity of the nucleotides was evaluated on an analytical reverse-phase column system, in two solvent systems as described in Supplementary data. Finally, aqueous solutions of the products were passed through a Dowex 50WX8-200 ion-exchange resin Na^+-form column and the products were eluted with deionized water to obtain the corresponding sodium salts after freeze-drying.

2.5.1. Separation of Di-(5-OMe)-uridine 5′,5″-P^1,P^3,α-boranotriphosphate (20A and 20B)

The separation of analogue **20** diastereoisomers, **20A** and **20B**, was accomplished using a semipreparative reverse-phase Gemini 5u column and isocratic elution with 93:7 (A) 100 mM TEAA, pH 7: (B) CH_3CN at a flow rate of 5 mL/min. Fractions containing purified isomers [Rt 6.60 min (**20A**); 10.87 min (**20B**) isomer)] were collected and freeze-dried. Excess buffer was removed by repeated freeze-drying cycles, with the solid residue dissolved each time in deionized water. Diastereoisomers **20A** and **20B** were obtained in 45.2% overall yield (74.4 mg) after LC separation.

2.5.2. Characterization of Di-(5-OMe)-uridine 5′,5″-P^1,P^3,α-boranotriphosphate (20A)

^{1}H NMR (D_2O; 600 MHz): δ 7.32 (s, 1H, H-6$_A$), 7.31 (s, 1H, H-6$_B$), 6.00 (d, J = 6.3, 1H, H-1′$_A$), 5.98 (d, J = 5.9, 1H, H-1′$_B$), 4.39 (m, 4H, H-2′$_A$, H-2′$_B$, H-3′$_A$, H-3′$_B$), 4.24 (m, 4H, H-4′$_A$, H-4′$_B$, H-5′$_A$, H-5′$_B$), 4.21 (m, 1H, H-5″$_A$), 4.12 (m, 1H, H-5″$_B$), 3.78 (s, 6H, CH_{3A}, CH_{3B}), 0.42 (m, 3H, BH_3) ppm. ^{31}P NMR (240 MHz, D_2O) δ: 84.29 (m, 1P, P_α-BH_3), −11.03 (d, J = 18.3 Hz, 1P, P_γ), −22.52 (dd, J = 27.8, J = 18.3 Hz, 1P, P_β) ppm. HR MALDI (negative) calcd for $C_{20}H_{31}B_1N_4O_{21}P_3$ 767.078 found 767.079. Purity data obtained on an analytical column: 96.8% and 95.1% purity using solvent system I and II, respectively.

2.5.3. Characterization of Di-(5-OMe)-uridine 5′,5″-P^1,P^3,α-boranotriphosphate (20B)

^{1}H NMR (D_2O; 600 MHz): δ 7.31 (s, 1H, H-6$_A$), 7.29 (s, 1H, H-6$_B$), 5.99 (d, J = 6.3, 1H, H-1′$_A$), 5.98 (d, J = 5.9, 1H, H-1′$_B$), 4.36 (m, 4H, H-2′$_A$, H-2′$_B$, H-3′$_A$, H-3′$_B$), 4.26 (m, 5H, H-4′$_A$, H-4′$_B$, H-5′$_A$, H-5′$_B$, H-5″$_A$), 4.08 (m, 1H, H-5″$_B$), 3.78 (s, 6H, CH_{3A}, CH_{3B}), 0.48 (m, 3H, BH_3) ppm. ^{31}P NMR (240 MHz, D_2O) δ: 84.05 (m, 1P, P_α-BH_3), −11.09 (d, J = 18.3 Hz, 1P, P_γ), −22.55 (dd, J = 31.4, J = 18.3 Hz, 1P, P_β) ppm. HR MALDI (negative) calcd for $C_{20}H_{31}B_1N_4O_{21}P_3$ 767.078 found 767.079. Purity data obtained on an analytical column: retention time: 97.3% and 95.9% purity using solvent system I and II, respectively.

2.6. Preparation of Di-(5-OMe)-uridine 5′,5″-P^1,P^3, triphosphate (21)

Tri-*n*-butylammonium-tri-*n*-octylammonium 5-OMe-uridine monophosphate salt (160.8 mg, 0.18 mmol) was dissolved in dry DMF (0.7 mL), and added to a flame-dried, nitrogen-flushed two-neck round bottom flask containing CDI (145.8 mg, 0.9 mmol, 5 equiv). The reaction was stirred at rt. After 2 h TLC (isopropanol:25% NH_4OH:H_2O 11:2:7) showed the presence of a less polar product (R_f 0.62) and the complete disappearance of the starting material (R_f 0.35). MeOH (0.06 mL, 1.62 mmol, 9 equiv) was added to destroy CDI leftovers, and, after 10 min, a solution of the tetra-*n*-butylammonium 5-OMe-uridine diphosphate, **8**, (0.18 mmol, 1 equiv) in dry DMF (0.5 mL) and $MgCl_2$ (68.4 mg, 0.72 mmol, 4 equiv) were added. The solution was stirred at rt and TLC monitoring after 24 h showed the presence of a more polar product (R_f 0.39) and the complete disappearance of intermediate, **30**. The solution was freeze-dried after the addition of water. The semisolid obtained after freeze-drying was chromatographed on an activated Sephadex DEAE-A25 column. The resin was washed with deionized water and loaded with the crude reaction residue dissolved in a minimal volume of water. The separation was monitored by UV detection (ISCO, UA-6) at 280 nm A buffer gradient of 0–0.2 M NH_4HCO_3 (250 mL of each solution) followed by a second buffer gradient of 0.2–0.4 M NH_4HCO_3 (300 mL of each solution) were applied. The different fractions were pooled and freeze-dried three times to yield a white solid. Final purification of the relevant fractions was carried out on an HPLC system, using a semi-preparative reverse-phase column, under the conditions described below. The purity of the nucleotides was evaluated on an analytical reverse-phase column, in two solvent systems as described in Supplementary data. Finally, aqueous solutions of the products were passed through a Dowex 50WX8-200 ion-exchange Na^+-form resin

column and the products were eluted with deionized water to obtain the corresponding sodium salts after freeze-drying.

2.6.1. Purification of Di-(5-OMe)-uridine 5′,5″-P¹,P³, triphosphate (21)

Purification of analogue **21** was accomplished using a semipreparative reverse-phase Gemini 5u column and isocratic elution with 96:4 (A) 100 mM TEAA, pH 7: (B) CH_3CN at a flow rate of 5 mL/min. The fraction containing the purified analogues (Rt 11.3 min) was collected and freeze-dried. Excess buffer was removed by repeated freeze-drying cycles, with the solid residue dissolved each time in deionized water. Analogue **21** was obtained in 51.8% overall yield (76.6 mg) after LC separation.

2.6.2. Characterization of Di-(5-OMe)-uridine 5′,5″-P¹,P³, triphosphate (21)

^{1}H NMR (D_2O; 600 MHz): δ 7.29 (s, 2H, H-6), 5.97 (d, J = 5.2, 2H, H-1′), 4.37 (m, 4H, H-2′, H-3′), 4.23 (m, 6H, H-4′, H-5′, H-5″), 3.77 (s, 6H, CH_3) ppm. ^{31}P NMR (240 MHz, D_2O) δ: −0.89 (d, J = 18.0 Hz, 1P, P_α), −22.26 (dd, J = 18.3, J = 18.0 Hz, 1P, P_β) ppm. HR MALDI (negative) calcd for $C_{20}H_{28}N_4O_{22}P_3$ 769.041 found 769.045. Purity data obtained on an analytical column: 97.2% and 97.4% purity using solvent system I and II, respectively.

2.7. Preparation of Di-(5-OMe)-uridine 5′,5″-P¹,P³,β-boranotriphosphate (22)

Tri-*n*-butylammonium-tri-*n*-octylammonium 5-OMe-uridine monophosphate salt (401.9 mg, 0.45 mmol) was dissolved in dry DMF (2 mL), and added to a flame-dried, nitrogen-flushed two-neck round bottom flask containing CDI (364.5 mg, 2.25 mmol, 5 equiv). The reaction was stirred at rt. After 2 h TLC (isopropanol:25% NH_4OH:H_2O 11:2:7) showed the presence of a less polar product (R_f 0.62) and the complete disappearance of the starting material (R_f 0.35). MeOH (0.09 mL, 2.25 mmol, 5 equiv) was added in order to destroy CDI leftovers, and, after 10 min, a solution of BPi (523.7 mg, 1.125 mmol, 2.5 equiv) in dry DMF (0.5 mL) and $MgCl_2$ (342.7 mg, 3.6 mmol, 8 equiv) were added. The solution was stirred at rt and TLC monitoring after 24 h showed the presence of more polar products and the complete disappearance of intermediate. The solution was freeze-dried after the addition of water. The semisolid obtained after freeze-drying was chromatographed on an activated Sephadex DEAE-A25 column. The resin was washed with deionized water and loaded with the crude reaction residue dissolved in a minimal volume of water. The separation was monitored by UV detection at 280 nm. A buffer gradient of 0–0.2 M NH_4HCO_3 (200 mL of each solution) followed by a second buffer gradient of 0.2–0.4 M NH_4HCO_3 (300 mL of each solution) were applied. The relevant fractions were pooled and freeze-dried three times to yield a white solid. Final purification of the relevant fractions was carried out on an HPLC system, using a semi-preparative reverse-phase column, under the conditions described below. The purity of the nucleotides was evaluated on an analytical reverse-phase column system, in two solvent systems as described in Supplementary data. Finally, aqueous solutions of the products were passed through a Dowex 50WX8-200 ion-exchange Na^+-form resin column and the products were eluted with deionized water to obtain the corresponding sodium salts after freeze-drying.

2.7.1. Purification of di-(5-OMe)-uridine 5′,5″-P¹,P³,β-boranotriphosphate (22)

Purification of analogue **22** was accomplished using a semi-preparative reverse-phase Gemini 5u column and isocratic elution with 96:4 (A) 100 mM TEAA, pH 7: (B) CH_3CN at a flow rate of 5 mL/min. The fractions containing the purified analogues (Rt 6.13 min) were collected and freeze-dried. Excess buffer was removed by repeated freeze-drying cycles, with the solid residue dissolved each time in deionized water. Analogue **22** was obtained in 8% overall yield (30.8 mg) after LC separation.

2.7.2. Characterization of Di-(5-OMe)-uridine 5′,5″-P¹,P³,β-boranotriphosphate (22)

^{1}H NMR (D_2O; 600 MHz): δ 7.30 (s, 1H, H-6), 6.00 (m, 2H, H-1′), 4.39 (m, 4H, H-2′, H-3′), 4.21 (m, 6H, H-4′, H-5′, H-5″), 3.78 (s, 6H, CH_3), 0.48 (m, 3H, BH_3) ppm. ^{31}P NMR (240 MHz, D_2O) δ: 80.43 (m, 1P, P_α-BH_3), −7.16 (d, J = 29.48 Hz, 1P, P_β) ppm. HR MALDI (negative) calcd for $C_{20}H_{31}B_1N_4O_{21}P_3$ 767.078 found 767.079. Purity data obtained on an analytical column: 96.3% and 96.1% purity using solvent system I and II, respectively.

2.8. Stability assays

2.8.1. General

For the chemical stability assays, ^{31}P NMR spectra were recorded (isotope frequency of 240 MHz). NPP 1 and 3 enzymes were provided by Professor Jean Sevigny (Center of Research in Rhumatology and Immunology, Laval University, Québec, Canada). Human blood serum was obtained from a blood bank (Tel-Hashomer Hospital, Israel). All stability experiments were performed in duplicates.

2.8.1.1. Evaluation of the chemical stability of analogues 4, 8, 18A and 31A. The stability of analogues **4**, **8**, **18A** and **31A** pH 1.4 was evaluated by ^{31}P NMR at 37 °C for monitoring possible dephosphorylation products. NMR spectra were recorded on a Bruker DMX-600 spectrometer with a ^{31}P NMR probe (isotope frequency of 240 MHz) using 85% H_3PO_4 as an external reference. Sodium salts of analogues **4**, **8**, **18A** and **31A** were dissolved in 0.45 mL of KCl/HCl buffer (pH 1.4) and D_2O (0.05 mL) was added. The final pH was adjusted to pH 1.4. pH measurements were performed with an Metrohm pH electrode and a Metrohm 827 pH lab pH meter. Spectra were recorded at 15 min, 1 h, or 24 h time intervals at 37 °C. For experiments that were several days long, the solution was kept in an oil bath at 37 °C and spectra were recorded at ca. 24 h time intervals. The phosphate ester hydrolysis rate was determined by measuring the change of the integration of one of the phosphates signals of the starting material with time.

2.8.1.2. Evaluation of resistance to of analogues 4, 8 and 18A degradation by NPP1,3. Evaluation of the activity of human NPP1 and NPP3 using *para*-nitrophenyl thymidine 5′-monophosphate (pnp-TMP) as a substrate, was performed as previously described.[48] Next, the percentage of hydrolysis of analogues **4**, **8** and **18A** by NPP1,3 was evaluated as follows: 56.15 μg or 57.78 μg of human NPP1 or NPP3 extract, respectively, was added to 0.575 mL the incubation mixture (1 mM $CaCl_2$, 200 mM NaCl, 10 mM KCl and 100 mM Tris, pH 8.5) and pre-incubated at 37 °C for 3 min. Reaction was initiated by the addition of 0.015 mL of 4 mM of each analogue (**4**, **8** or **18A**). The reaction was stopped after 2 h or 3 h NPP1 or NPP3, respectively, by transferring a 0.1 mL aliquot from the reaction mixture to 0.350 mL ice-cold 1 M perchloric acid. These samples were centrifuged for 1 min at 10,000×*g*. Supernatants were neutralized with 170 μL 2 M KOH in 4 °C and centrifuged 1 min at 10,000×*g*. The reaction mixture was filtered and freezed-dried. The hydrolysis rates of the analogues **4**, **8** and **18A** by NPP1 or NPP3 were determined by measuring the change in the integration of the HPLC peaks for each analogue over time versus control. The percentage of compound degradation was calculated versus control, to take into consideration the degradation of the compounds due to the addition of acid to stop the enzymatic reaction. Therefore, each of the samples was compared to a control which was transferred to acid, but to which

no enzyme was added. The percentage of degradation was calculated from the area under the curve of the nucleoside monophosphate peak, after subtraction of the control, which is the amount of the nucleoside monophosphate peak formed due to chemical acidic hydrolysis.

2.8.1.3. Evaluation of the stability of analogues 4, 8, 18A and 31A in human blood serum. The assay mixture containing 0.1 mg each analogue in deionized water (4.5 μL), human blood serum (180 μL), and RPMI-1640 medium (540 μL)[49] was incubated at 37 °C for 0–24 h. At 0.5–12 h intervals each sample was heated to 80 °C for 30 min, treated with CM Sephadex (1–2 mg), shaken for 2 h, centrifuged for 6 min (12,000 rpm), and the aqueous layer was collected and extracted with chloroform (2 × 500 μL). The aqueous layer was freeze-dried and then dissolved in deionized water (100 μL). Samples were loaded onto an activated Starta X-AW weak anion exchange cartridge, washed with H_2O (1 mL) and eluted with MeOH:H_2O (1:1, 1 mL) followed by NH_4OH:MeOH:H_2O (2:25:73, 1 mL), and then freeze-dried. The resulting residue was analyzed by HPLC on a Gemini analytical column (5 μ C-18 557 110A; 150 mm × 4.60 mm), using gradient elution with solvent system I (for analogues **4** and **8**—A:B 96:4 over 10 min) or II (for **18A** or **31A**—A:B 97.5:2.5 over 10 min) at a flow rate of 1 mL/min. The hydrolysis rates of the analogues **4**, **8**, **18A** and **31A** with blood serum were determined by measuring the change in the integration of the HPLC peaks for each analogue over time versus control. The percentage of compound degradation was calculated versus control, to take into consideration the degradation of the compounds due to the work up following the enzymatic reaction. Therefore, each of the samples was compared to a control which was put through the same workup, but to which no serum was added. The percentage of degradation was calculated from the area under the curve of the nucleoside monophosphate peak, after subtraction of the control, which is the amount of the nucleoside monophosphate peak formed due to chemical hydrolysis.

2.9. Evaluation of activity of analogues 18A/B and 20A/B, 21 and 22 at $P2Y_{2/4/6}$ receptors

2.9.1. Cell culture and transfection

GFP (green fluorescent protein) constructs of human $P2Y_2$-R, $P2Y_4$-R and $P2Y_6$-R were stably expressed in 1321N1 astrocytoma cells, which lack endogenous expression of P2X- and P2Y-receptors. The respective cDNA of the receptor gene was cloned into a pEGFPN1 vector and after transfection, using FuGENE 6 Transfection Reagent (Roche Molecular Biochemicals, Mannheim, Germany), cells were selected with 0.5 mg/mL G418 (geneticine; Merck Chemicals, Darmstadt, Germany) and grown in Dulbecco's modified Eagles' medium (DMEM) supplemented with 10% fetal calf serum (FCS), 100 U/mL penicillin and 100 U/mL streptomycin at 37 °C and 5% CO_2. The expression and cell membrane localization of the respective P2Y receptors was confirmed through the analysis of the GFP fluorescence. The functionality of the expressed GFP-labeled receptor in cells was verified by recording a change of $[Ca^{2+}]_i$ after stimulation with the appropriate receptor agonist.

2.9.2. Single cell calcium measurements

1321N1 Astrocytoma cells transfected with the respective plasmid for P2Y-R-GFP expression plated on coverslips (22 mm diameter) and grown to approximately 80% density, were incubated with 2 μM fura 2/AM and 0.02% pluronic acid in Na-HBS buffer (Hepes buffered saline: 145 mM NaCl, 5.4 mM KCl, 1.8 mM $CaCl_2$, 1 mM $MgCl_2$, 25 mM glucose, 20 mM Hepes/Tris pH 7.4) for 30 min at 37 °C. The cells were superfused (1 mL/min, 37 °C) with different concentrations of nucleotide in Na-HBS buffer. The nucleotide-induced change of $[Ca^{2+}]_i$ was monitored by detecting the respective emission intensity of fura 2/AM at 510 nm with 340 nm and 380 nm excitations.[50] The average maximal amplitude of the responses and the respective standard errors were calculated from ratio of the fura 2/AM fluorescence intensities with excitations at 340 nm and 380 nm. We only analyzed GFP-labeled cells. Microsoft Excel (Microsoft Corp., Redmond, WA, USA) and SigmaPlot (SPSS Inc., Chicago, IL, USA) were used to derive the concentration–response curves and EC_{50} values from the average response amplitudes obtained in at least three independent experiments.[51,52] Only cells with a clear GFP-signal and with the typical calcium response kinetics upon agonist pulse application were included in the data analysis. The GFP-tagged P2Y receptors are suitable for pharmacological and physiological studies, as previously reported.[53–55]

The activity of analogues **19A/B** was tested in another laboratory in a slightly different method, see Supplementary data (S5).

3. Results and discussion

3.1. Design of uracil nucleotides as potential $P2Y_6$-R agonists

Recently, we reported that 5-OMe-UDP **8** displayed increased potency and selectivity at the $P2Y_6$, receptor as compared to **4**.[16] Therefore, here we used **8** as a scaffold for improving the pharmacological properties of **4**. In an attempt to overcome the inherent instability of nucleotide based drug candidates, we combined two approaches known to improve the stability of nucleotides: (1) the application of a dinucleotide scaffold. This scaffold is known to be metabolically more stable than the corresponding nucleotide. (2) the application of isoster-based (e.g. boranophosphate isosters) non-hydrolyzable nucleotides. Previously, we demonstrated the beneficial pharmacological properties of borano-phosphate isosters by a series of potent and selective $P2Y_1$-R agonists, based on boranophosphate isosters of ATP analogues (adenosine-5′-α-borano-triphosphate analogues).[23,38] The borane group introduces a chiral center, thus resulting in a pair of diastereoisomers. We observed that the absolute configuration of the agonist determines the receptor subtype selectivity. The adenosine-5′-α-borano-triphosphate analogues proved to be highly stable at physiological pH and relatively stable at pH 1.4 and 37 °C as compared to the parent compound.[23] Furthermore, they were found to be relatively resistant to enzymatic hydrolysis by e-NTPDase.[23]

Therefore, here we designed a novel series of $P2Y_6$-R agonists bearing one or two modifications at two sites of the **4** or Up_3U scaffold. Both scaffolds bear three negative charges required for recognition by $P2Y_6$-R.[11,39] Specifically, compounds **18**–**22**, were synthesized, bearing a methoxy modification at the C5 position of the uracil ring and a boranophosphate modification at either P_α or P_β position of the nucleotide or dinucleotide analogue (Fig. 3).

3.2. Synthesis of potential $P2Y_6$-R ligands

3.2.1. Synthesis of analogues 18–22

5-OMe-uridine mono- and di-phosphate (**23** and **8**, respectively) were synthesized from 5-OMe-uridine, **24**, as previously described.[16,44,45,47]

Methoxymethylidene protected uridine analogue, **25**,[46] was used for the synthesis of 5-OMe-uridine-5′-*O*-(α-boranodiphosphate), **18**, by a one-pot phosphorylation reaction (Scheme 1).[23,56,57] First, 2-Cl-1,3,2-benzdioxaphosphorin-4-one and dry pyridine in dry dioxane were added to protected uridine, **25**, in DMF to generate intermediate **26**. After stirring at rt for 10 min, tributylammonium pyrophosphate salt in dry DMF was added to form the cyclic intermediate **27**, followed by the addition of a 2 M solution of

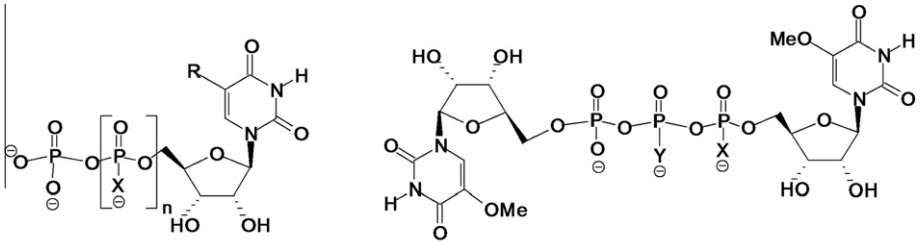

8 X = O n = 1 R = OMe
18 A/B X = BH_3 n = 1 R = OMe
19 A/B X = BH_3 n = 2 R = OMe
31 A/B X = BH_3 n = 1 R = H

20 A/B X = BH_3 Y = O
21 X = O Y = O
22 X = O Y = BH_3

Figure 3. 5-OMe-uridine nucleotide and dinucleotide analogues studied here.

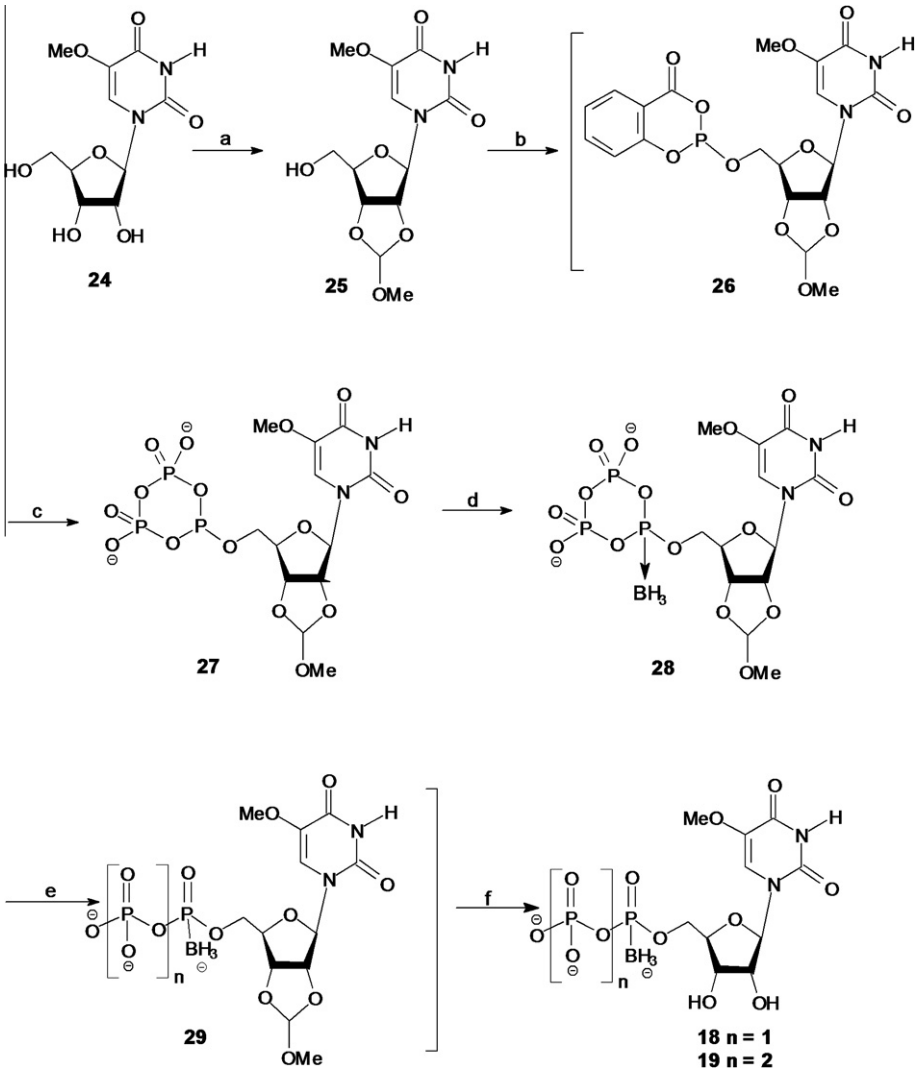

Scheme 1. Reagents and conditions: (a) (1) $HC(OMe)_3$, *p*-TsOH, rt, overnight; and (2) Dowex (weak base), rt, 3 h, 96%; (b) 2-Cl-1,3,2-benzdioxaphosphorin-4-one, dry DMF, dry dioxane, rt, 10 min; (c) 1 M $P_2O_7H_2^{2-}(Bu_3N^+H)_2$ in dry DMF, Bu_3N, rt, 5 min; (d) 2 M $BH_3{\cdot}SMe_2$ in THF, rt, 15 min; (e) ethylenediamine, rt, 10 min; (f) (1) 10% HCl, pH 2.3, rt, 3 h; and (2) 24% NH_4OH, pH 9, rt, 45 min, 51% and 9% of **18** and **19**, respectively. (diastereoisomers mixtures after LC separation).

$BH_3{\cdot}SMe_2$ complex in THF leading to intermediate **28**. Subsequently, ethylenediamine was added to generate **29**. Finally, the reaction was quenched with water, and the clear solution was evaporated and freeze-dried. The removal of the methoxymethylidene group involved a hydrolysis step at pH 2.3 and then at pH 9. Analogue **18** was obtained in a 51% yield, with **19** as a byproduct from the hydrolysis of intermediate **28** in 9% yield.

For the synthesis of analogues **20** and **21**, analogue **23** was activated with CDI to generate the P-donor[58] and analogues **18** and **8** served as P-acceptors, respectively. $MgCl_2$ was added to the

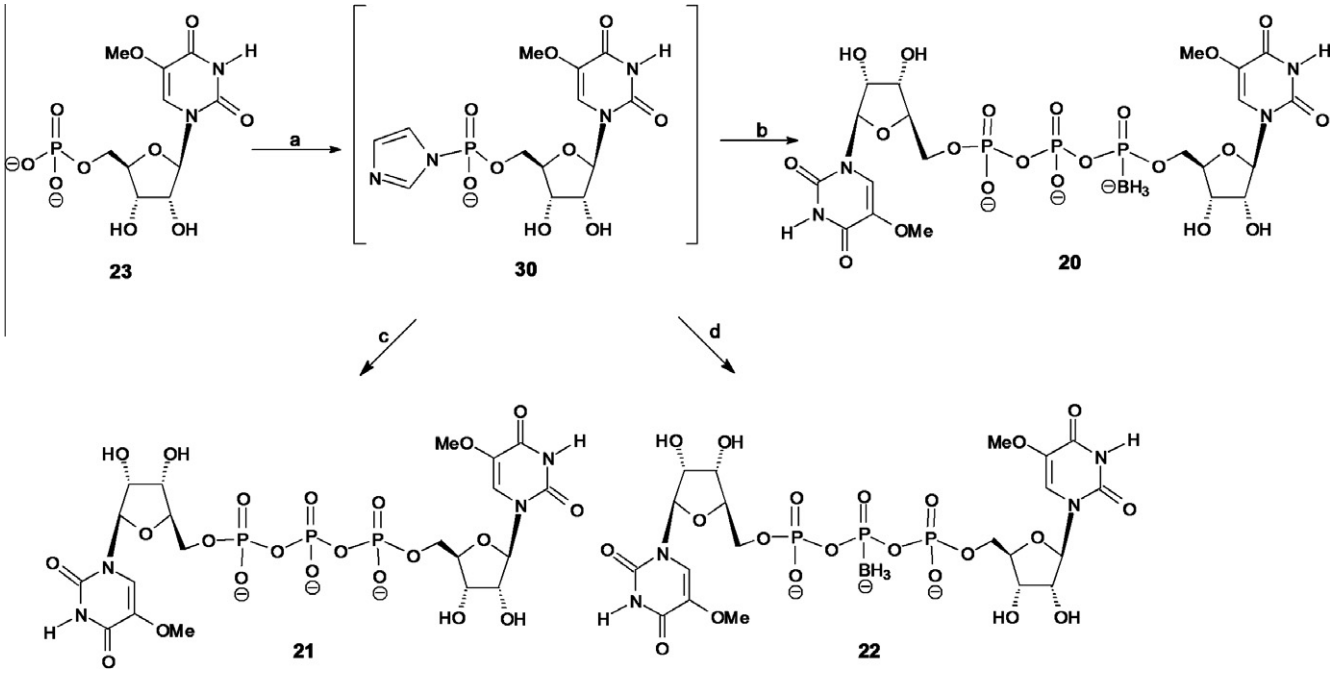

Scheme 2. Reagents and conditions: (a) carbodiimidazole, dry DMF, rt, 2.5 h (b) (1) dry MeOH, rt, 5 min; and (2) **18** in dry DMF, $MgCl_2$, rt, overnight, 45% (yield after LC separation). (c) (1) dry MeOH, rt, 10 min; and (2) **18** in dry DMF, $MgCl_2$, rt, overnight, 52% (after LC separation). (d) (1) dry MeOH, rt, 10 min; and (2) BPi in dry DMF, $MgCl_2$, rt, overnight, 8% (yield after LC separation).

reaction mixtures because phosphoroimidazolide was reported to be most reactive in the presence of divalent metal ions.[59] Briefly, tri-*n*-butylammonium, tri-*n*-octylammonium salt of 5-OMe-uridine-monophosphate, **23**, was activated with carbonyl di-imidazole (CDI) in dry DMF at rt to yield **30**, followed by the addition of the nonactivated nucleotides, that is, tris(tributylammonium) salts of 5-OMe-uridine-5′-*O*-(α-boranodiphosphate), **18**, or 5-OMe-uridine diphosphate, **8**, in dry DMF in the presence of $MgCl_2$ (Scheme 2), to produce analogues **20** and **21** in a 45% and 52% yield, respectively.

Recently, we reported the synthesis of several diadenosine and diuridine tri- and penta(borano)phosphate analogues.[59] We used this method for the synthesis of di-(5-OMe)-uridine 5′,5″-P^1,P^3,α-boranotriphosphate, **22**. Briefly, the synthesis involved the activation of 2 equiv tri-*n*-butylammonium, tri-*n*-octylammonium salt of 5-OMe-uridine monophosphate, **23**, with CDI in dry DMF, followed by the addition of 1 equiv boranophosphate (BPi) in DMF and $MgCl_2$ to produce analogue **22** in an 8% yield (Scheme 2).

Purification of all new analogues included ion-exchange LC followed by final purification and diastereomers separation (in the case of analogues **18–20**) by HPLC.

3.3. Assignment of the absolute configuration of analogues 18–20

We have shown that some P2Y receptors are activated by only one of the diastereomers of borano-substituted nucleotides.[38,51] Therefore, we separated the two diastereomers of each of the chiral analogues (**18–20**) before evaluating them as $P2Y_6$-R agonists and determined their absolute configuration based on their ^{1}H NMR spectra.[38]

The two diastereoisomers of **18** exhibited different chemical shifts of H5′ proton (δ 4.30 vs 4.25 ppm). Likewise, H5″ proton chemical shifts of both **18** diastereomers were different from the corresponding proton of the non-chiral analogue **8** (δ 4.09 vs 4.18 ppm). The only **18** rotamer in which different chemical shifts can be expected for H5′/H5″ protons is the *gg* rotamer, both around the C4′–C5′ and the C5′–O5′ bonds (Fig. 4). The small, although indicative, Δδ between H5″ of both **18** isomers (δ 4.09 ppm) as compared to the non-borano derivative, **8** (δ 4.18 ppm), may be explained in terms of the greater proximity of the negative charge on BH_3 (in **18**) to H5″ (Fig. 4A/B), as compared to O (in **8**) (Fig. 4C). The δ of H5′ in A isomer versus B isomer of **18** (δ 4.30 vs 4.25 ppm) and

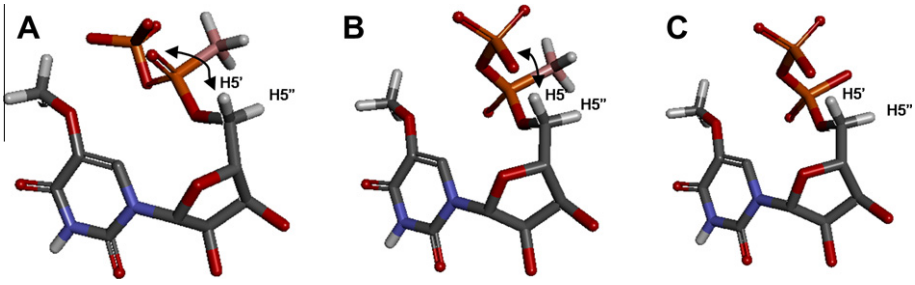

Figure 4. Absolute configuration assignment of **18**. (A) R_p configurations of **18A**. (B) S_p configurations of **18B**. (C) Non-chiral analogue, **8**.

Table 1
Potencies (EC_{50} in μM) of nucleotides and dinucleotides **18–22** at the $P2Y_2$-R, $P2Y_4$-R and $P2Y_6$-R in 1321N1 astrocytoma cells

Agonist	EC_{50} values of nucleotides (μM)		
	$P2Y_2$-R	$P2Y_4$-R	$P2Y_6$-R
3	0.14 ± 0.04	0.9 ± 0.4	—
4	—	—	0.15 ± 0.03
8	n.d.r.[a]	⩾20	0.08 ± 0.009[16]
18A	n.d.r.	n.d.r.	0.008 ± 0.003
18B	n.d.r.	n.d.r.	4.3 ± 1.9
19A	n.d.r.	n.d.r.	11.23 ± 0.63
19B	n.d.r.	n.d.r.	20.11 ± 0.70
20A	n.d.r.	n.d.r.	0.06 ± 0.02
20B	n.d.r.	n.d.r.	2.2 ± 0.5
21	n.d.r.	n.d.r.	>10[b]
22	n.d.r.	n.d.r.	0.2 ± 0.04

[a] n.d.r. = no detectable response for nucleotide concentrations of up to 100 μM.
[b] For nucleotide concentrations of up to 100 μM it was not possible to calculate an EC_{50} value, since the plateau of the rise of $[Ca^{2+}]_i$ was not reached.

versus the H5′ chemical shift of **8** (δ 4.22 ppm), can be explained by its relative proximity to whichever group is on P_α. This group is either a non-resonating oxygen (in R_p configuration) (Fig. 4A), or negatively charged oxygen atoms PO_3^- (P_β) in S_p configuration (Fig. 4B). The shielding effect of the negatively charged oxygen atoms on P_β as compared to the less negative non-resonating oxygen on P_α results in different chemical shifts for H5′ of either isomer. Therefore, H5′ of A isomer, which is closer to the oxygen on P_α, is less shielded and appears more downfield than B isomer. Thus, the R_p configuration can be attributed to A-isomer, **18A**, and S_p to B-isomer, **18B**. Assuming the same order of elution in HPLC, the absolute configuration assignment for the other chiral analogues, **19**, **20**, and **31**, is the same as for **18**.

3.4. Evaluation of uridine nucleotide analogues 18–22 as $P2Y_{2/4/6}$-Rs ligands

To study the activity of nucleotides **18–22** at the $P2Y_{2/4/6}$-Rs, we evaluated $[Ca^{2+}]_i$ mobilization induced by these analogues and compared it to that of **3** and **4**. These studies were performed in 1321N1 astrocytoma cells that were stably transfected with $P2Y_{2/4/6}$ receptors. Concentration–response curves were derived for a range of nucleotide concentrations, usually from 10^{-8} M to at least 10^{-5} M and in some cases, up to 10^{-4} M when possible. The results are shown in Supplementary data (Fig. S1) and summarized in Table 1. In control measurements, we found that untransfected 1321N1 astrocytoma cells did not show a response to any of the tested nucleotides (Fig. 5C).

Analogues **18–22** showed no activity at both $P2Y_2$-R and $P2Y_4$-R. All analogues except **21** displayed some activity at the $P2Y_6$-R. The most potent compounds found were **18A** and **20A**. At the $P2Y_6$ receptor, there is a clear preference for **18** A-isomer over **18** B-isomer (EC_{50} 0.008 μM and 4.3 μM, respectively). Compound **18A** was found to be 500-times more potent than **18B** and 19-times more potent than **4** (EC_{50} 0.15 μM), thus making it the most potent $P2Y_6$-R agonist currently known. Both isomers of the triphosphate analogue, **19A/B**, showed poor agonist activity at $P2Y_6$-R (EC_{50} 11.23 and 20.11 μM, respectively, data not shown). The potency of **20** A-isomer (EC_{50} 0.06 μM) is 2.5-times higher than that of **4**, and the potency of the B-isomer is far lower (EC_{50} 2.2 μM). The diastereoisomeric preferences of the $P2Y_6$ receptor for dinucleotides **20A** and **B** are less pronounced than for **18A/B**, but also noticeable. The parent compound **8** did show a biphasic concentration–response curve in our previous publication.[16] However, the analysis of the new compounds **18A/B** and **20A/B** did not display an indication for comparable biphasic behavior. The EC_{50} value of **21** is expected to be >10 μM (Supplementary data, Fig. S1C). Dinucleotide **22** showed a comparable potency to that of **4** (EC_{50} 0.15 μM). The order of potencies of nucleotides **18–22** at the $P2Y_6$-R in 1321N1 astrocytoma cells is as follows: **18A** > **20A** > **4** = **22** > **20B** > **18B** > **19A** > **19B** > **21**. All tested nucleotides were completely inactive at the $P2Y_2$-R and $P2Y_4$-R in transfected 1321N1 cells and at 1321N1 wild-type cells. In addition, these nucleotides did not evoke any response at 1321N1 wild-type cells (Fig. 5). Thus, from our data we can definitely conclude that the newly developed nucleotides are selective at activating the $P2Y_6$ receptor, when compared with the $P2Y_2$ and $P2Y_4$ receptor. Yet, we cannot exclude that the studied nucleotide analogues may be active at $P2Y_{14}$-R, as this receptor was recently reported to be activated by **4**.[2]

The potency and selectivity of analogues **18–22** at $P2Y_6$-R led us to some SAR observations:

3.4.1. Borano substitution at P_α of a uridine nucleotide/dinucleotide increases significantly agonist potency at the $P2Y_6$-R

The introduction of a chiral center in **8**, by BH_3-substitution of non-bridging oxygen at P_α, reveals a stereo-selectivity of the receptor for the A-isomer over the B-isomer. The preference of $P2Y_6$-R for R_p isomer has not been observed previously. However, we have already described diastereoselective properties of $P2Y_1$- and $P2Y_{11}$-receptors which displayed preference for the R_p and S_p isomers of borano-phosphate and phosphorothioate adenine nucleotides, respectively.[38,51] Based on our computational studies of $P2Y_1$-R, we previously suggested that a Mg^{2+} ion, which is bound to the nucleotide inside the receptor, binds the P_α oxygen atom in

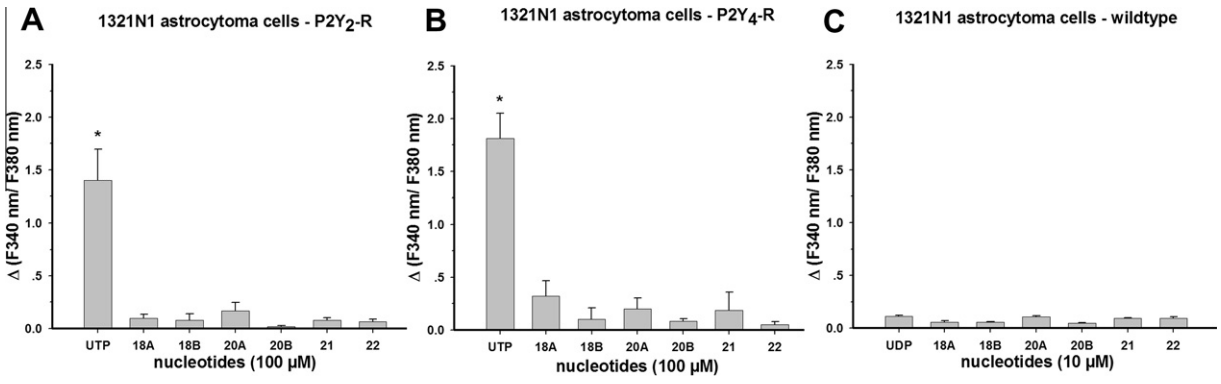

Figure 5. Rise of $[Ca^{2+}]_i$ in 1321N1 astrocytoma cells (A: $P2Y_2$-R, B: $P2Y_4$-R, C: wild-type) after treatment with 100 μM of the newly synthesized nucleotides on A and B and 10 μM on C. Cells were pre-incubated with 2 μM fura-2 AM for 30 min and change in fluorescence (δ F340 nm/F380 nm) was detected. * = The statistical significance level between the standard agonist **3** and each of the newly synthesized nucleotides is P <0.001.

ATP-α-B analogues, rather than the borane group. Thus, in the ATP-α-B (S_p) isomers, the P_α oxygen is not in a position to coordinate the Mg^{2+} ion, and in this case, the coordination occurs probably via $P_{\beta,\gamma}$. Hence, this isomer loses a tight interaction, possibly with Mg^{2+} ion, resulting eventually in its higher EC_{50} values.[38] Similarly, we assume that analogue **18B** (S_p isomer) is less potent than **18A** (R_p isomer) due to the loss of the binding interactions of $P2Y_6$-R with P_α of **18B.**

Although borano-substitution enhanced dramatically the potency of **8** at $P2Y_6$-R, the corresponding triphosphate mono-nucleotide**, 19**, was hardly active at the $P2Y_6$-R. This inactivity was due to the preference of the receptor for three phosphate negative charges.[11,39] Likewise, at the $P2Y_2$-R **19** was completely inactive, even though this compound is similar to the receptor's endogenous agonist, **3**. The inactivity of **19** as opposed to the activity of 5-OMe-UTP at $P2Y_2$-R (EC_{50} 2 μM, compared to **3**, EC_{50} 0.1 μM),[16] implies that $P2Y_2$-R does not tolerate the P_α-borano group. This observation was already made before for ATP(α-B) which elicited a very weak response at the $P2Y_2$ receptor, as compared to the endogenous ligands **1** and **3**.[53]

3.4.2. Borano-dinucleotide analogues 20–22 are less potent than the corresponding mono-nucleotide analogue 18

The decrease in activity of dinucleotide **20A** versus mono-nucleotide **18A** is possibly due to the requirement for a terminal phosphate for molecular recognition by $P2Y_6$-R. Even so, **20A** is still more active than **21** or **22,** since **20A** is structurally more similar to **18A**. The least active $P2Y_6$-R agonist is **21** which is the dinucleotide bearing two methoxy substitutions, one on each of the uracil rings. Surprisingly, this analogue was less active at $P2Y_6$-R than the previously reported dinucleotide triphosphate, Up_3U. Apparently, the double 5-OMe substitution in dinucleotide **21** noticeably reduced the potency at the $P2Y_6$ receptor (Supplementary data, Fig. S1). Nevertheless, similarly to the mono-nucleotides, the beneficial effect of the borano group in enhancing potency at the $P2Y_6$-R is evident: all borano-bearing nucleotides, either at P_α or P_β were far more active than their non-borano counterparts—**18A** versus **8**, and **20A** and **22** versus **21**.

3.5. Chemical and enzymatic stability of 18A

To evaluate the potential of **18A**, the most potent agonist found here, as a drug candidate targeting $P2Y_6$-R, we subjected **18A** to several stability tests as described below.

3.5.1. Hydrolytic stability of 18A at acidic pH

We evaluated the chemical stability of **18A** and compared it to related control analogues—**4**, **8** and **31A**. The hydrolytic stability of each analogue was monitored under conditions simulating gastric juice acidity (pH 1.4 and 37 °C) using KCl/HCl buffer. The method of choice for monitoring the hydrolysis of borano-analogues, **18A** and **31A**, was ^{31}P NMR spectrometry, since the signal of the phosphate hydrolysis products is at ca. 0 ppm, while that of the boranophosphate analogues **18A** and **31A** is at ca. 85 ppm. Spectra were recorded at 15 min, 1 h, or 24 h time intervals at 37 °C. The phosphate ester hydrolysis rate was determined by measuring the changes in the integration of one of the phosphate signals of **18A** with time, and was fit to a pseudo-first-order reaction model (Fig. 6A).

During the hydrolysis of **18A**, we first observed a signal of inorganic phosphate emerging at 0.62 ppm, together with a signal for the remaining boranophosphate of 5-OMe-UMPα-B) at 96.57 ppm. At the same time, the signals for P_β (−10.69 ppm) and P_α (86.55 ppm) of the **18A** decreased, indicating that the terminal phosphate was rapidly lost under these conditions. Next, two additional signals appeared at 7.31 and 4.42 ppm, indicating the formation of the 5-OMe-uridine-H-phosphonate and inorganic H-phosphonate moieties, respectively (Fig. 6B). The rate constant of $1.31 \times 10^{-5}\ s^{-1}$ ($t_{1/2}$ = 16.9 h) was established for **18**, as compared with $6.66 \times 10^{-7}\ s^{-1}$ ($t_{1/2}$ = ∼12 days), $6.25 \times 10^{-7}\ s^{-1}$ ($t_{1/2}$ = ∼13 days) and $1.14 \times 10^{-5}\ s^{-1}$ ($t_{1/2}$ = 16.8 h) for **4**, **8**, and, **31A**, respectively.

3.5.2. Resistance of analogue 18A to hydrolysis by NPP1,3

Next, we explored resistance of analogue **18A** to enzymatic hydrolysis at isolated NPPs, namely, NPP1,3, which are some of the major enzymes responsible for the hydrolysis of extracellular nucleotides.

We determined the hydrolysis rate of analogue **18A** by each enzyme after incubation at 37 °C in the appropriate buffer for 2 or 3 h (for NPP1 and NPP3, respectively) as compared to **4** and **8**. The enzymatic reaction was stopped by adding the reaction mixture into ice-cold perchloric acid. The stability of **4** and analogues **8** and **18A** to hydrolysis by NPPs was determined by measuring the change in the integration of the HPLC peaks for each analogue as compared to control. The percentage of compound degradation was calculated versus control, to take into consideration the degradation of the compounds due to the addition of acid to stop the enzymatic reaction. Therefore, each of the samples was compared to a control which was transferred to acid, but to which no enzyme was added. The percentage of degradation was calculated from the area under the curve of the nucleoside monophosphate peak, after subtraction of the control. This percentage is the amount of the nucleoside monophosphate peak formed due to chemical acidic hydrolysis.

In the presence of NPP1, **4** was 50% hydrolyzed to UMP after 2 h of incubation with the enzyme. Analogue **8** was similarly hydrolyzed to 5-OMe-UMP (49%). Yet, analogue **18A** was only 15% hydrolyzed after the same incubation time. Analogue **18A** exhibited relative stability also regarding to hydrolysis by NPP3. This stability is compared to analogues **4** and **8** undergoing 28% and 45%, 36% hydrolysis, respectively, with the corresponding nucleoside 5′-monophosphates after incubation of 3 h (Table 2).

3.5.3. Resistance of analogue 18A to hydrolysis in human blood serum

The usage of nucleoside-5′-triphosphates for therapeutic purposes is limited due to their rapid dephosphorylation in extracellular media. Four major families of ectonucleotidases have been identified: (1) NTPDases; (2) NPPs; (3) the glycosylphosphatidylinositol (GPI)-anchored ecto-5′-nucleotidase, and (4) the GPI-anchored alkaline phosphatase (AP).[22]

Blood serum contains dephosphorylating enzymes and, therefore, provides a good model system for the estimation of the in vivo stability of nucleotide analogues. Previous studies have used human blood serum[60] to demonstrate the metabolic stability of phosphonate modified nucleotide analogues.[31,33,34,49,61]

We determined the half-life of analogue **18A** in human blood serum as compared to **4**, **8** and **31A**. These analogues were incubated in human blood serum and RPMI-1640 at 37 °C for 0.5–24 h. The stability of analogues **18A**, **4**, **8** and **31A** in human blood serum was determined by measuring the change in the integration of the HPLC peaks for each analogue over time. The percentage of compound degradation was calculated versus control (similarly to the described above for NPP).

Compound **4** was hydrolyzed to UMP, followed by further degradation to uridine, with a half-life of 2.4 h. Yet, analogue **8** was hydrolyzed to the corresponding nucleoside 5′-monophosphate and nucleoside with a half-life of 11.9 h, and analogue **31A** displayed a half-life of 21 h. Compound **18A** was hydrolyzed to

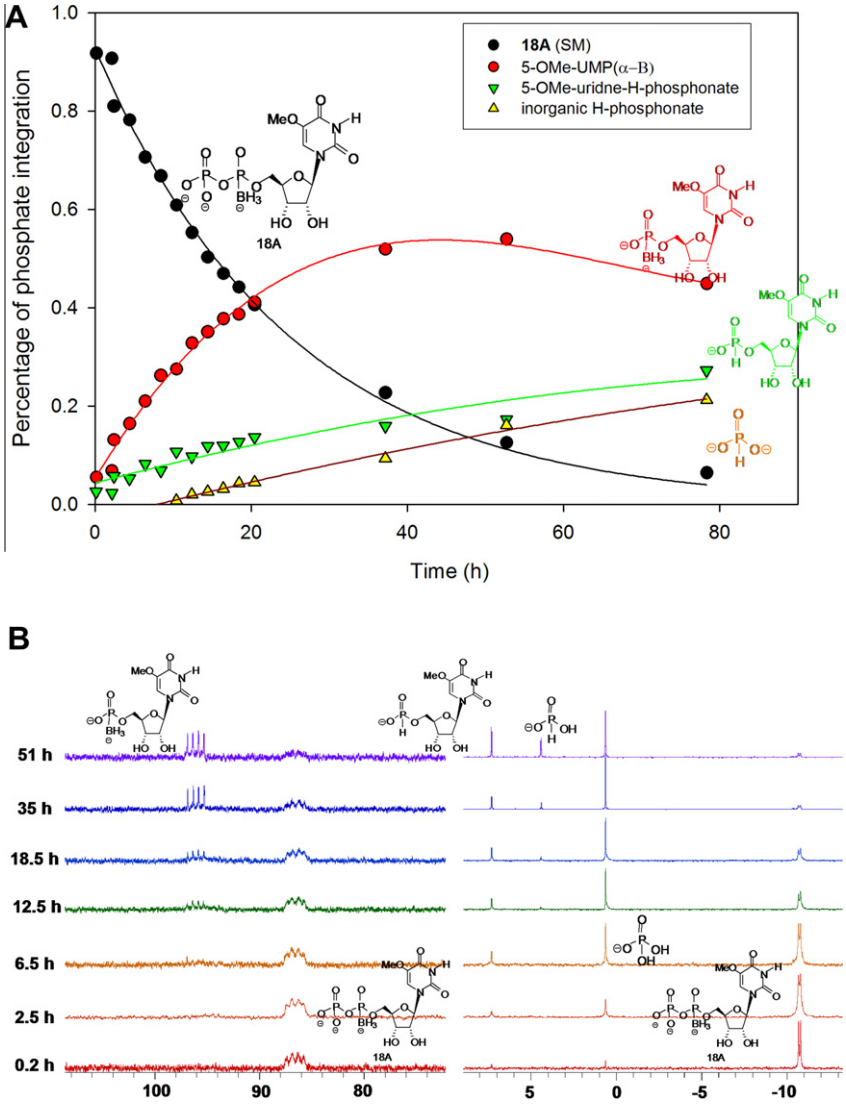

Figure 6. (A) Rate of hydrolysis of **18A** under gastric-juice acidity conditions monitored by ^{31}P NMR at 240 MHz. The different curves represent the time-dependent species concentration due to hydrolysis of **18A**: (a) Black—**18A** (starting material); (b) Red—5-OMe-UMP(α-B); (c) Green—5-OMe-uridine-H-phophonate; (d) Yellow—inorganic H-phosphonate. (B) Time-dependent ^{31}P NMR spectra (240 MHz) of hydrolysis of **18A** trisodium salt in KCl/HCl solution (pH 1.4 and 37 °C).

Table 2
Hydrolysis percentage of analogues **4**, **8** and **18A** by NPP1,3

Analogue	Hydrolysis percentage[a,b]	
	NPP1	NPP3
4	50% ± 3	45% ± 1
8	49% ± 1	36% ± 7
18A	15% ± 5	28% ± 1

[a] After incubation at 37 °C in buffer (1 mM $CaCl_2$, 200 mM NaCl, 10 mM KCl and 100 mM Tris, pH 8.5) for 2 or 3 h, with NPP1 or NPP3, respectively.
[b] Values represent mean ± S.D. of two experiments (P <0.05).

5-OMe-UMP(α-B), and then to 5-OMe-uridine with a half-life of 17 h (Fig. 7).

We concluded that the introduction of a borano group at the P_α position of UDP analogues affects their chemical and metabolic stability as follows: **(A)** P_α Borano substitution reduces the stability of **18A** versus UDP, **4**, under conditions simulating gastric juice acidity. The reduction of chemical stability observed for borano-bearing analogues **18A** and **8** is explained by the susceptibility of the

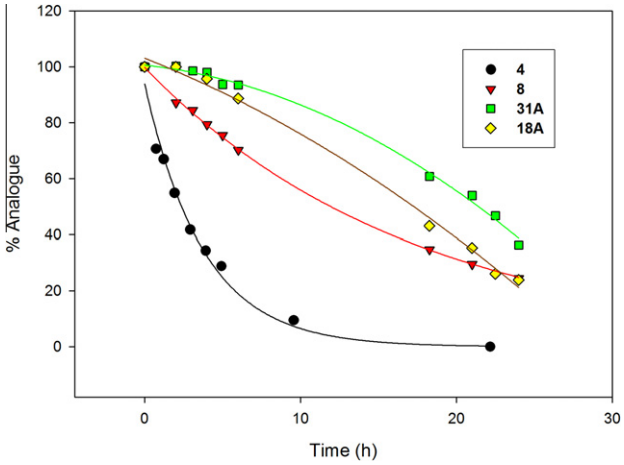

Figure 7. Time-dependent hydrolysis of **4** and analogues **8**, **18A**, and **31A** in human blood serum (180 μL) and RPMI-1640 medium (540 μL) over 24 h at 37 °C, as monitored by HPLC.

P–B bond to acidic hydrolysis, as compared to that of the P–O bond.[42] Even so, a half-life of 16.9 h is quite satisfactory for a drug candidate. **(B)** The BH_3 substitution at P_α position increases resistance to degradation by NPP1,**3**. The introduction of the boranophosphate moiety at P_α plays an important role in protecting UDP analogues against NPP1,3 hydrolysis. The enzymatic degradation by NPP occurs between P_α and P_β. Yet, since BH_3 group in analogue **18A** is larger than O in the parent compound, it possibly prevents an attack by an essential water molecule on P_α and makes these analogues poor NPP substrates. Furthermore, analogue **8**, bearing only a modification at the uracil ring, was hydrolyzed more slowly by NPP3, but not by NPP1 as compared to **4**. **(C)** The BH_3 substitution at P_α position and OMe at the C5 position of uracil nucleotides increase resistance to degradation in human blood serum. The methoxy group presents a steric hindrance which causes analogue **8** to be a poor substrate for the various enzymes present in blood serum. Apparently, the borano group in analogues **18A** and **31A** renders the nucleotides even more stable to enzymatic degradation than **4**.

3.6. Conclusions

To date, only very few synthetic nucleotides were reported to be more potent than the endogenous agonist, **4**, at the $P2Y_6$-R. Here, we identified 5-OMe-UDP(α-B) R_p isomer, **18A**, as the most potent and selective agonist at the $P2Y_6$-R currently known, being 19-fold more potent than **4**. The combination of two substitutions—a methoxy at the UDP C5 position and a BH_3 group at the P_α position, which presented another chiral center—greatly increased the agonist activity of the previously discovered agonist **8**. Compound **18A** exhibits a half-life of 16.9 h under conditions simulating gastric juice acidity, and improved resistance to enzymatic degradation by NPP1 and NPP3 as compared to UDP, **4**, (15% vs 50% and 28% vs 45% degradation, respectively). Furthermore, the borane group induced a sevenfold increased stability ($t_{1/2}$ 17 h) in human blood serum as compared to the endogenous $P2Y_6$-R agonist, **4** ($t_{1/2}$ 2.4 h). The beneficial pharmacological properties of **18A** prompted us to explore its therapeutic potential, which will be reported in due course.

Supplementary data

Supplementary data associated with this article can be found, in the online version, at http://dx.doi.org/10.1016/j.bmc.2012.07.042.

References and notes

1. Jacobson, K. A.; Boeynaems, J. M. *Drug Discov. Today* **2010**, *15*, 570.
2. Carter, R. L.; Fricks, I. P.; Barrett, M. O.; Burianek, L. E.; Zhou, Y.; Ko, H.; Das, A.; Jacobson, K. A.; Lazarowski, E. R.; Harden, T. K. *Mol. Pharmacol.* **2009**, *76*, 1341.
3. Bar, I.; Guns, P.-J.; Metallo, J.; Cammarata, D.; Wilkin, F.; Boeynams, J.-M.; Bult, H.; Robaye, B. *Mol. Pharmacol.* **2008**, *74*, 777.
4. Koizumi, S.; Shigemoto-Mogami, Y.; Nasu-Tada, K.; Shinozaki, Y.; Ohsawa, K.; Tsuda, M.; Joshi, B. V.; Jacobson, K. A.; Kohsaka, S.; Inoue, K. *Nature (London U. K.)* **2007**, *446*, 1091.
5. Grbic, D. M.; Degagne, E.; Langlois, C.; Dupuis, A.-A.; Gendron, F.-P. *J. Immunol.* **2008**, *180*, 2659.
6. Kim, S. G.; Gao, Z.-G.; Soltysiak, K. A.; Chang, T.-S.; Brodie, C.; Jacobson, K. A. *Cell. Mol. Neurobiol.* **2003**, *23*, 401.
7. Mamedova, L. K.; Wang, R.; Besada, P.; Liang, B. T.; Jacobson, K. A. *Pharmacol. Res.* **2008**, *58*, 232.
8. Balasubramanian, R.; de Azua, I. R.; Wess, J.; Jacobson, K. A. *Biochem. Pharmacol.* **2010**, *79*, 1317.
9. Markovskaya, A.; Crooke, A.; Guzman-Aranguez, A. I.; Peral, A.; Ziganshin, A. U.; Pintor, J. *Eur. J. Pharmacol.* **2008**, *579*, 93.
10. El-Tayeb, A.; Qi, A.; Muller, C. E. *J. Med. Chem.* **2006**, *49*, 7076.
11. Jacobson, K. A.; Ivanov, A. A.; Castro, S.; Harden, T. K.; Ko, H. *Purinergic Signal.* **2009**, *5*, 75.
12. Costanzi, S.; Joshi, B. V.; Maddileti, S.; Mamedova, L.; Gonzalez-Moa, M. J.; Marquez, V. E.; Harden, T. K.; Jacobson, K. A. *J. Med. Chem.* **2005**, *48*, 8108.
13. Maruoka, H.; Barrett, M. O.; Ko, H.; Tosh, D. K.; Melman, A.; Burianek, L. E.; Balasubramanian, R.; Berk, B.; Costanzi, S.; Harden, T. K.; Jacobson, K. A. *J. Med. Chem.* **2010**, *53*, 4488.
14. Besada, P.; Shin, D. H.; Costanzi, S.; Ko, H.; Mathe, C.; Gagneron, J.; Gosselin, G.; Maddileti, S.; Harden, T. K.; Jacobson, K. A. *J. Med. Chem.* **2006**, *49*, 5532.
15. Brunschweiger, A.; Muller, C. E. *Curr. Med. Chem.* **2006**, *13*, 289.
16. Ginsburg-Shmuel, T.; Haas, M.; Schumann, M.; Reiser, G.; Kalid, O.; Stern, N.; Fischer, B. *J. Med. Chem.* **2010**, *53*, 1673.
17. Ko, H.; Carter, R. L.; Cosyn, L.; Petrelli, R.; de Castro, S.; Besada, P.; Zhou, Y.; Cappellacci, L.; Franchetti, P.; Grifantini, M.; Van Calenbergh, S.; Harden, T. K.; Jacobson, K. A. *Bioorg. Med. Chem.* **2008**, *16*, 6319.
18. Nicholas, R. A.; Watt, W. C.; Lazarowski, E. R.; Li, Q.; Harden, T. K. *Mol. Pharmacol.* **1996**, *50*, 224.
19. Korcok, J.; Raimundo, L. N.; Du, X.; Sims, S. M.; Dixon, S. J. *J. Biol. Chem.* **2005**, *280*, 16909.
20. Kim, H. S.; Ravi, R. G.; Marquez, V. E.; Maddileti, S.; Wihlborg, A.-K.; Erlinge, D.; Malmsjoe, M.; Boyer, J. L.; Harden, T. K.; Jacobson, K. A. *J. Med. Chem.* **2002**, *45*, 208.
21. Mamedova, L. K.; Joshi, B. V.; Gao, Z.-G.; von Kugelgen, I.; Jacobson, K. A. *Biochem. Pharmacol.* **2004**, *67*, 1763.
22. Zimmerman, H. *Naunyn-Schmiedeberg's Arch. Pharmacol.* **2000**, *362*, 299.
23. Nahum, V.; Zuendorf, G.; Levesque, S. A.; Beaudoin, A. R.; Reiser, G.; Fischer, B. *J. Med. Chem.* **2002**, *45*, 5384.
24. Grobben, B.; Claes, P.; Roymans, D.; Esmans, E. L.; Van Onckelen, H.; Slegers, H. *Br. J. Pharmacol.* **2000**, *130*, 139.
25. Zimmermann, H. *Drug Dev. Res.* **2001**, *52*, 44.
26. Blackburn, G. M.; Taylor, G. E.; Thatcher, G. R. J.; Prescott, M.; McLennan, A. G. *Nucleic Acids Res.* **1987**, *15*, 6991.
27. Kowalska, J.; Lewdorowicz, M.; Darzynkiewicz, E.; Jemielity, J. *Tetrahedron Lett.* **2007**, *48*, 5475.
28. Lin, J.; Porter, K. W.; Shaw, B. R. *Nucleos. Nucleot. Nucleic Acids* **2001**, *20*, 1019.
29. Misiura, K.; Szymanowicz, D.; Stec, W. J. *Org. Lett.* **2005**, *7*, 2217.
30. Cusack, N. J.; Hourani, S. M. O.; Loizou, G. D.; Welford, L. A. *Br. J. Pharmacol.* **1987**, *90*, 791.
31. Eliahu, S. E.; Camden, J.; Lecka, J.; Weisman, G. A.; Sevigny, J.; Gelinas, S.; Fischer, B. *Eur. J. Med. Chem.* **2009**, *44*, 1525.
32. Joseph, S. M.; Pifer, M. A.; Przybylski, R. J.; Dubyak, G. R. *Br. J. Pharmacol.* **2004**, *142*, 1002.
33. Boyle, N. A.; Rajwanshi, V. K.; Prhavc, M.; Wang, G.; Fagan, P.; Chen, F.; Ewing, G. J.; Brooks, J. L.; Hurd, T.; Leeds, J. M.; Bruice, T. W.; Cook, P. D. *J. Med. Chem.* **2005**, *48*, 2695.
34. Eliahu, S.; Martin-Gil, A.; Perez de Lara, M. J.; Pintor, J.; Camden, J.; Weisman, G. A.; Lecka, J.; Sévigny, J.; Fischer, B. *J. Med. Chem.* **2010**, *53*, 3305.
35. Holy, A. *Curr. Pharm. Des.* **2003**, *9*, 2567.
36. De Clercq, E.; Holy, A. *Nat. Rev. Drug Discov.* **2005**, *4*, 928.
37. Zhou, Z.; Wang, X.; Li, M.; Sohma, Y.; Zou, X.; Hwang, T.-C. *J. Physiol.* **2005**, *569*, 447.
38. Major, D. T.; Nahum, V.; Wang, Y.; Reiser, G.; Fischer, B. *J. Med. Chem.* **2004**, *47*, 4405.
39. Shaver, S. R.; Rideout, J. L.; Pendergast, W.; Douglass, J. G.; Brown, E. G.; Boyer, J. L.; Patel, R. I.; Redick, C. C.; Jones, A. C.; Picher, M.; Yerxa, B. R. *Purinergic Signal.* **2005**, *1*, 183.
40. Yerxa, B. R.; Sabater, J. R.; Davis, C. W.; Stutts, M. J.; Lang-Furr, M.; Picher, M.; Jones, A. C.; Cowlen, M.; Dougherty, R.; Boyer, J.; Abraham, W. M.; Boucher, R. C. *J. Pharmacol. Exp. Ther.* **2002**, *302*, 871.
41. http://www.businesswire.com/news/home/20110103005364/en, Access date: 11.12.2011.
42. Nahum, V.; Fischer, B. *Eur. J. Inorg. Chem.* **2004**, 4124.
43. Burnstock, G.; Fischer, B.; Hoyle, C. H. V.; Maillard, M.; Ziganshin, A. U.; Brizzolara, A. L.; von Isakovics, A.; Boyer, J. L.; Harden, K.; Jacobson, K. A. *Drug Dev. Res.* **1994**, *31*, 206.
44. Niedballa, U.; Vorbruggen, H. *J. Org. Chem.* **1976**, *41*, 2084.
45. Stout, M. G.; Robins, R. K. *J. Heterocycl. Chem.* **1972**, *9*, 545.
46. Griffin, B. E.; Jarman, M.; Reese, C. B.; Sulston, J. E. *Tetrahedron* **1967**, *23*, 2301.
47. Chesterfield, J. H.; McOmie, J. F. W.; Tute, M. S. *J. Chem. Soc.* **1960**, 4590.
48. Levesque, S. A.; Lavoie, E. G.; Lecka, J.; Bigonnesse, F.; Sevigny, J. *Br. J. Pharmacol.* **2007**, *152*, 141.
49. Eliahu, S.; Barr, H. M.; Camden, J.; Weisman, G. A.; Fischer, B. *J. Med. Chem.* **2010**, *53*, 2472.
50. Ubl, J. J.; Vöhringer, C.; Reiser, G. *Neuroscience* **1998**, *86*, 597.
51. Ecke, D.; Tulapurkar, M. E.; Nahum, V.; Fischer, B.; Reiser, G. *Br. J. Pharmacol.* **2006**, *149*, 416.
52. Ecke, D.; Hanck, T.; Tulapurkar, M. E.; Schäefer, R.; Kassack, M.; Stricker, R.; Reiser, G. *Biochem. J.* **2008**, *409*, 107.
53. Tulapurkar, M. E.; Laubinger, W.; Nahum, V.; Fischer, B.; Reiser, G. *Br. J. Pharmacol.* **2004**, *142*, 869.
54. Tulapurkar, M. E.; Zundorf, G.; Reiser, G. *J. Neurochem.* **2006**, *96*, 624.
55. Zylberg, J.; Ecke, D.; Fischer, B.; Reiser, G. *Biochem. J.* **2007**, *405*, 277.
56. Li, P.; Xu, Z.; Liu, H.; Wennefors, C. K.; Dobrikov, M. I.; Ludwig, J.; Shaw, B. R. *J. Am. Chem. Soc.* **2005**, *127*, 16782.
57. Ludwig, J.; Eckstein, F. *J. Org. Chem.* **1991**, *56*, 1777.
58. Hoard, D. E.; Ott, D. G. *J. Am. Chem. Soc.* **1965**, *87*, 1785.
59. Nahum, V.; Tulapurkar, M.; Levesque Sebastien, A.; Sevigny, J.; Reiser, G.; Fischer, B. *J. Med. Chem.* **1980**, *2006*, 49.
60. Arzumanov, A. A.; Semizarov, D. G.; Victorova, L. S.; Dyatkina, N. B.; Krayevsky, A. A. *J. Biol. Chem.* **1996**, *271*, 24389.
61. Wang, G.; Boyle, N.; Chen, F.; Rajappan, V.; Fagan, P.; Brooks, J. L.; Hurd, T.; Leeds, J. M.; Rajwanshi, V. K.; Jin, Y.; Prhavc, M.; Bruice, T. W.; Cook, P. D. *J. Med. Chem.* **2004**, *47*, 6902.